Chemical Science

ROYAL SOCIETY OF CHEMISTRY

EDGE ARTICLE

View Article Online
View Journal

Cite this: DOI: 10.1039/d5sc06490b

All publication charges for this article have been paid for by the Royal Society of Chemistry

Received 25th August 2025
Accepted 20th February 2026

DOI: 10.1039/d5sc06490b

rsc.li/chemical-science

Triple threat bismuth peptide imaging in cells

Saan Voss, †[a] Clinton J. Kidman, †[b] Liam D. Adair, [cd] Samuel O. Nitschke, [cd] Pramsak Patawanich, [cd] Terry Koh, [b] Ani T. Baker, [b] Daryl L. Howard, [e] Elizabeth J. New, [cd] Hugh H. Harris *[b] and Christoph Nitsche *[a]

Bismuth peptides are emerging as a novel class of pharmaceutical agents. While cell-penetrating bismuth peptides have been reported recently, their detailed cellular interactions and stability remain poorly understood, and therefore new methods are required to visualise these peptides within cells. In this study, we synthesised cell-penetrating bismuth peptides conjugated to various fluorescent dyes (naphthalimide, coumarin, rhodamine B) and their brominated analogues, and investigated their cellular uptake in SKOV-3 cells using X-ray fluorescence microscopy (XFM) for bismuth and bromine, alongside optical fluorescence microscopy. Co-localisation of bromine, bismuth and the fluorescent dyes within the cytosol and cellular compartments indicates that the bismuth-peptide conjugates can enter cells intact. Among the three fluorescent dyes tested, naphthalimide and its brominated derivative were the most robust for multimodal imaging.

Introduction

Bismuth peptides are an emerging class of structurally constrained molecules with potential for pharmaceutical applications. Coordination with bismuth enables the formation of defined bicyclic or tricyclic topologies, locking peptides into bioactive conformations and enhancing overall stability. For example, enzyme substrate sequences can be transformed into nanomolar inhibitors with improved resistance to proteolytic degradation.[1] Similarly, basic peptide motifs can be used to generate bicyclic cell-penetrating peptides (CPPs) that outperform conventional linear CPPs.[2,3] The conformational rigidity introduced by bismuth coordination enhances target affinity and improves pharmacokinetic properties, including increased plasma stability.[4] Genetically encoded libraries based on phage display allow high-throughput identification of specific bismuth peptides for proteins of interest,[5,6] expanding their scope in biomedical research.

Bismuth peptides are constructed by incorporating three cysteine residues into a peptide of interest which tightly coordinate Bi(III).[1] If the starting peptide is linear, this coordination results in a bicyclic structure with two loops (Fig. 1). In contrast, tricyclic peptides can be generated by introducing bismuth coordination into pre-existing macrocyclic peptides with three cysteine residues binding one Bi(III) atom.[4] A fundamental advantage of constraining peptides with bismuth over conventional organic scaffolds, such as the alkylating agent tris(bromomethyl)benzene,[7,8] is that bismuth can also serve a functional role. For example, bismuth isotopes can be used in

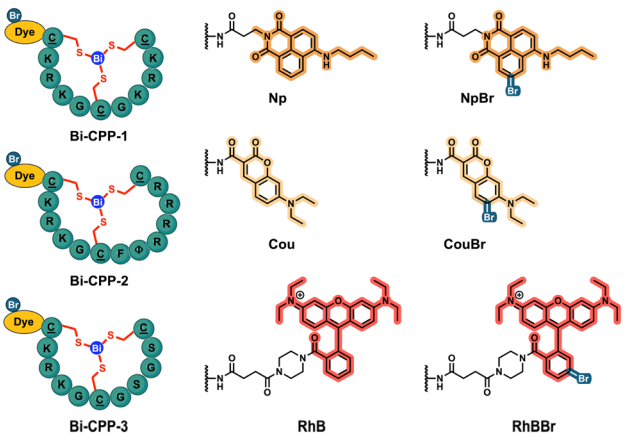

Fig. 1 Bismuth cell-penetrating bicyclic peptides (Bi-CPPs) used in this study, along with fluorescent dyes, both with and without an additional bromine label. All peptides contain a C-terminal amide and bind bismuth *via* three cysteine residues (C). Fluorescent dyes were directly attached to the N-terminus, while peptides without a dye were N-terminally acetylated. Np, naphthalimide; Cou, coumarin; RhB, rhodamine B; NpBr, brominated naphthalimide; CouBr, brominated coumarin; RhBBr, brominated rhodamine B; Φ, L-3-(2-naphthyl) alanine.

[a]Research School of Chemistry, College of Science and Medicine, Australian National University, Canberra, ACT 2601, Australia. E-mail: christoph.nitsche@anu.edu.au
[b]Discipline of Chemistry, The University of Adelaide, North Terrace, Adelaide, SA 5005, Australia. E-mail: hugh.harris@adelaide.edu.au
[c]School of Chemistry, The University of Sydney, Sydney, NSW, 2006, Australia
[d]Australian Research Council Centre of Excellence for Innovations in Peptide and Protein Science, The University of Sydney, Sydney, NSW, 2006, Australia
[e]Australian Synchrotron, ANSTO, 800 Blackburn Road, Clayton, VIC 3168, Australia
† These authors contributed equally.

targeted alpha therapy to destroy cancer cells,[9] or as tracers to monitor cellular uptake.[2,10]

When we recently explored bismuth cell-penetrating peptides (Bi-CPPs), we leveraged the labelling capacity of the bismuth centre by analysing cellular uptake using ICP-MS of cell lysates, in addition to conventional fluorescence labelling with rhodamine B.[2] However, this approach cannot distinguish between true cellular uptake and material that remains associated with the cell membrane, nor can it provide spatial resolution regarding the intracellular localisation. Fluorescence labelling, in turn, can confirm the intracellular location of the peptide but cannot determine whether it remains coordinated to bismuth or if the dye has been cleaved.

To overcome limitations in tracking bismuth peptides within human cells, which is relevant for their future biomedical application, we developed a multimodal labelling strategy that enables direct imaging of bismuth alongside orthogonal labels. We previously demonstrated that bismuth peptides exhibit strong *in vitro* stability against cellular competitors such as glutathione (GSH).[2,4] To further evaluate the robustness of the Bi–S coordination motif under conditions that more closely mimic the *in vivo* environment, we synthesised a set of bismuth peptides functionalised for multimodal imaging (Fig. 1).[11] These constructs were designed to be compatible with both optical fluorescence microscopy and X-ray fluorescence microscopy (XFM), allowing simultaneous visualisation of peptide localisation and bismuth distribution in cultured cells. These methods are complementary, enabling localisation of both optically fluorescent moieties appended to the peptides and heavier elements, including bismuth and bromine, within the same sample.

Results and discussion

Designing multimodal cell-penetrating bismuth peptides

We employed three different Bi-CPPs, which were previously shown to penetrate HeLa cells at sub-micromolar concentrations (Fig. 1).[2] All peptides contain a KRKG motif in the N-terminal loop, which we earlier associated with enhanced uptake *via* macropinocytosis.[2] The three peptides differ in their C-terminal loop. **Bi-CPP-1** contains an additional (G)KRK motif, **Bi-CPP-2** features a FΦRRRR sequence (where Φ represents L-3-(2-naphthyl)alanine), previously reported by Pei and co-workers,[12] and **Bi-CPP-3** includes a non-basic GSGS motif. Each loop of the peptide bicycles investigated in this study contains 4–6 amino acid residues between the cysteines that coordinate the bismuth atom. Multiple previous studies have demonstrated that loops containing 3–8 amino acids fall within a suitable range for the formation of stable peptide-bismuth bicycles.[1–6]

Our strategy was to use X-ray fluorescence microscopy to localise bismuth in cells following treatment with bismuth peptides and then compare this with the localisation of both the XFM bismuth signal and optical fluorescence when cells were treated with analogous, otherwise identical bismuth peptides labelled with three different fluorophores; naphthalimide, coumarin and rhodamine B (Fig. 1).

We have previously demonstrated correlative multimodal optical and X-ray fluorescence microscopy (XFM) in cells treated with bromine-labelled naphthalimides.[13] In this study, we applied the same approach by appending brominated fluorophores to a selection of bismuth peptides (Fig. 1). This set of compounds allowed us to compare the cellular distributions of bismuth and bromine, as detected by XFM, with the corresponding fluorescent signals. By directly correlating these data, we were able to determine whether bismuth remains coordinated to the peptides following cellular uptake and processing. In addition, mapping bismuth distribution enabled us to assess how different degrees of functionalisation, such as fluorophore type and bromination, influence the cellular handling and localisation of bismuth peptides.

Bromination of the fluorophores exhibited similar absorption and emission maxima and lower quantum yields compared to the non-brominated analogues (Table S1 and Fig. S1–S6). Quantum yields were sufficiently high for microscopy studies, with the brominated rhodamine B exhibiting particularly high quantum yields, even in aqueous solution.

In this work, we report imaging data for cultured human ovarian cells (SKOV-3) following a standard chemical fixation protocol that we have employed previously for XFM studies.[14] This facilitates multimodal data collection given the more stringent requirements for synchrotron XFM experimentation, but we note that live cell optical (confocal) imaging with our functionalised peptides is also feasible.[2] The impact of fluorescent labelling on cellular processing is assessed in this work. Five representative conjugates, covering all three CPPs and dyes explored, were evaluated for cytotoxicity using an MTT assay (Fig. S42), revealing no significant toxic effects at the concentration of 10 μM, which was used for all imaging experiments.

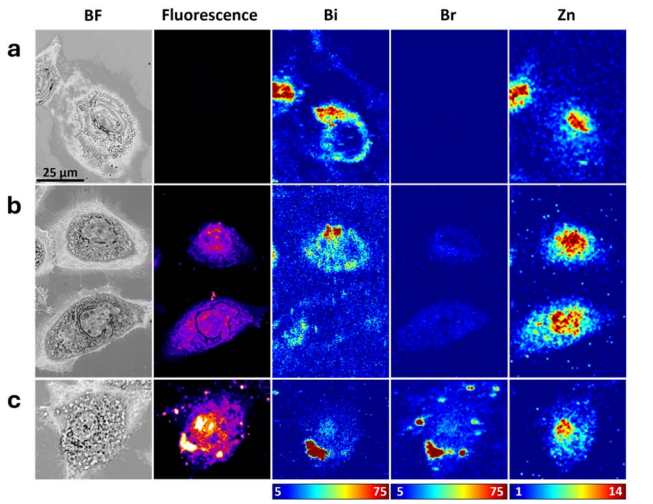

Fig. 2 Correlation of brightfield (BF), confocal optical fluorescence (naphthalimide) and XFM images (Bi, Br and Zn – false colour scale bars show areal density in ng cm^{-2}) for SKOV-3 cells treated with (a) **Bi-CPP-1**, (b) **Bi-CPP-1-Np** and (c) **Bi-CPP-1-NpBr** (all treatments 10 μM, 4 h). Scale bar at top left (25 μm) applies to all images.

Bi-CPP-1 conjugated to naphthalimide analogues

Fig. 2 shows images of representative cells treated with bismuth peptide **Bi-CPP-1**, followed by a naphthalimide-appended version, **Bi-CPP-1-Np**, and then a brominated naphthalimide-appended version of the same peptide, **Bi-CPP-1-NpBr**. Similar images of additional cells from the various treatments are presented in the SI (Fig. S28–S30). In some cells treated with **Bi-CPP-1** (*e.g.* Fig. 2a and 4a), XFM images indicate that bismuth displays a cytoplasmic distribution, localised outside the nucleus, which is represented by the corresponding cellular localisation of zinc. Conversely, several other cells show a correlation between bismuth and zinc distributions, suggesting the presence of bismuth in the nucleus. In these latter examples, the optical micrographs show confluent or overlapping cell bodies. Taken together with the fact that XFM images project three-dimensional structures onto two dimensions (meaning that material above or below the nucleus may appear coincident with it) we interpret the imaging data as indicating that bismuth from this peptide treatment predominantly accumulates in extranuclear, likely cytosolic, compartments or organelles.

The same windows were imaged by confocal fluorescence microscopy. The naphthalimide-labelled **Bi-CPP-1-Np** (Fig. 2b) showed a markedly enhanced signal at the emission wavelength appropriate for this fluorophore, compared to the signal observed in cells treated with the unlabelled bismuth peptide, **Bi-CPP-1** (Fig. 2a). In cells treated with the fluorophore-labelled peptide, **Bi-CPP-1-Np**, there is an apparent, although incomplete, correlation between the optical fluorescence distribution and that of bismuth as detected by XFM (Fig. 2b). The distribution of bismuth is phenomenologically similar to that observed in cells treated with the unlabelled bismuth peptide, **Bi-CPP-1**. The correlation between the bismuth and naphthalimide signal distributions is robust and generally intracellular, in that where one signal is evident, the other is also present. However, the relative intensities of the two signals vary.

It is important to recognise the differences in the imaging modalities used to generate the optical fluorescence and XFM images shown in Fig. 2 and subsequent Fig. 3–6, and to consider potential discrepancies when comparing them. As noted above, for XFM data the full depth of the imaged object is compressed into two dimensions, such that all elemental content is displayed in a single map. In contrast, the optical fluorescence images shown are taken from single confocal slices (with an apparent *z*-depth of approximately 1.88 μm). Therefore, discrepancies in the assessment of bismuth peptide distribution may arise when comparing XFM bismuth maps with naphthalimide or other fluorophore signal distributions, for example, in the lower cell in Fig. 2b.

We note that in some areas of samples treated with the fluorophore-labelled peptide, fluorescence signal is detected in small regions of the substrate where no visible cells or bismuth signal are present (*cf.* far right side of the naphthalimide signal panel in the top row of Fig. S29). This may indicate some cleavage of the fluorophore from the peptide, with or without involvement of cellular processing, leading to extracellular accumulation of the cleaved moiety.

Cells treated with the brominated fluorophore-labelled version **Bi-CPP-1-NpBr** show improved cellular uptake of the peptide, as indicated by the greater maximal areal density (in ng cm^{-2}) of bismuth in XFM maps and the more pronounced naphthalimide fluorescence signal within cells, compared to the treatments described above. These cells suggest the distribution of bismuth is variable and that some perinuclear and nuclear distribution is occasionally present, differing from other compounds (Fig. 2c and S30).

The inclusion of a bromine functional atom on the naphthalimide allows comparison of the bromine and bismuth elemental distributions, combined with the localisation of the optical fluorescence signal from naphthalimide. This comparison reveals a consistent correlation between the bromine distribution and naphthalimide fluorescence; however, the correlation between these signals and the distribution of bismuth is less distinct. The bismuth distribution generally correlated with cell bodies and with both the Br and naphthalimide distributions, but we note several accumulations of naphthalimide and bromine where bismuth was not evident, both intracellularly and extracellularly in substrate regions not associated with cells. This may again indicate partial cleavage of the fluorophore, now including bromine, from the peptide, but at present we cannot distinguish whether this involves uptake of the conjugate into cells (which would involve excretion to produce the extracellular bromine-naphthalimide correlated regions), or whether the cleavage occurs directly in media and outside of cells.

Introduction of the bromine functionality to the peptide conjugate led to a marked increase in intracellular bromine measured by XFM, in terms of both the observed maximal areal densities and the average bromine areal densities across several cells (Fig. 7b), when compared to the other two treatments in this **Bi-CPP-1** set. Bromine is present at trace levels in cell growth media (including serum additive), so detection in cells treated with non-brominated peptides was anticipated. However, we observed a marked and statistically significant increase in intracellular bromine in cells treated with the brominated naphthalimide-labelled peptide (**Bi-CPP-1-NpBr**).

Similarly, quantitation of the intracellular average bismuth areal density, calculated over many cells (~20 cells) and measured using XFM (Fig. 7a), indicated a statistically significant increase compared to controls, in which the bismuth content was assumed to be below the detection limit of the technique. The bismuth content did not vary significantly between cells treated with any of the three Bi-CPPs shown in Fig. 2.

Bi-CPP-2 conjugated to naphthalimide analogues

The same SKOV-3 cell line was then treated with an analogous set of peptides based on **Bi-CPP-2** (Fig. 1), with identical naphthalimide and brominated naphthalimide functionalities. Correlated brightfield, optical fluorescence micrographs and XFM elemental maps are shown in Fig. 3 and S31–S33 for cells

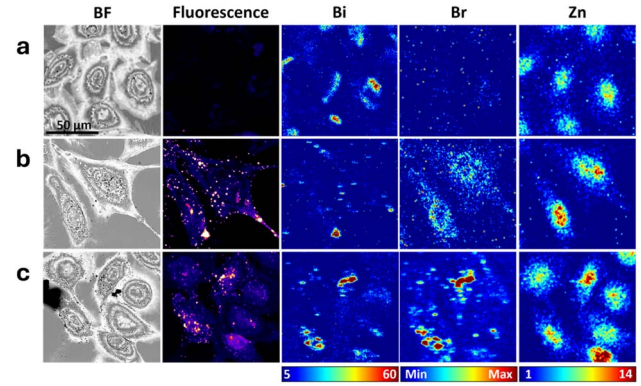

Fig. 3 Correlation of brightfield (BF), confocal optical fluorescence (naphthalimide) and XFM images (Bi, Br and Zn – false colour scale bars show areal density in ng cm^{-2}) for SKOV-3 cells treated with (a) **Bi-CPP-2**, (b) **Bi-CPP-2-Np** and (c) **Bi-CPP-2-NpBr** (all treatments 10 μM, 4 h). Scale bar at top left (50 μm) applies to all images. False colour intensity for XFM Br maps is (a and b) 1.5–8.5 ng cm^{-2} and (c) 5–75 ng cm^{-2}.

treated under these conditions. Comparison of images from this series of treatments to the analogous **Bi-CPP-1** (Fig. 2) reveals key similarities, along with several distinctions in the handling and accumulation of the peptides by the cells due to the different CPP sequences used. In the **Bi-CPP-2** series, treatment with the peptides led to accumulation of bismuth within cells and a significant increase in intracellular bismuth across all three treatment conditions. The bismuth distribution was strongly correlated with both the naphthalimide and bromine distributions when these components were present. Cellular bismuth was statistically elevated in all three treatments relative to controls. However, compared to the **Bi-CPP-1** set, we noted statistically significant variations in bismuth content between the three **Bi-CPP-2** samples (Fig. 7c). Compared to **Bi-CPP-1**, **Bi-CPP-2** contains one additional basic residue and two more residues overall. Treatment with the peptide lacking a fluorophore label led to a higher cellular bismuth content than either of the sets of cells treated with the labelled peptides. The underlying mechanism for this distinction is unclear, but we speculate that the extra hydrophobic moiety impacts on the cellular uptake mechanism, as this CPP already has a fine-tuned content of basic (charged) and hydrophobic (phenyl and naphthyl) residues.[3,12] Incorporation of a bromine atom into the peptide again led to a statistically significant elevation of intracellular bromine compared to the other two treatments, as assessed by XFM (Fig. 7d).

In all three treatments with the **Bi-CPP-2** set, the resulting cellular distribution of the peptides (assessed using the bismuth; bismuth and naphthalimide; and bismuth, bromine and naphthalimide signals, respectively) was more consistently localised within cells, compared to distributions observed in the **Bi-CPP-1** set, which is in line with previous studies that reported cytosolic release of bicyclic peptides bearing the FΦRRRR and related sequences.[3,12] The optical fluorescence and XFM data demonstrate a more consistent correlation of the various signals in the two fluorophore labelled peptide treatments, suggesting that these conjugates are more stable overall under these conditions, compared to the **Bi-CPP-1** set where we noted some indication for fluorophore cleavage.

Bi-CPP-1 conjugated to coumarin analogues

Due to its easier synthetic accessibility (absence of non-canonical amino acids) and its smaller overall size, we selected **Bi-CPP-1** to further investigate its effects and compatibility with alternative fluorescent dyes and their brominated variants. A third analogous set of peptides was prepared in which the naphthalimide fluorophore was replaced with a coumarin (Cou) moiety. Correlated multimodal images of cells treated with the respective members of this set are presented in Fig. 4, S34 and S35. XFM data collection for this experiment involved a shorter dwell time, resulting in decreased signal-to-noise. Bismuth was readily visualised within cells treated with each of these three compounds. The perinuclear distribution of bismuth observed in cells treated with **Bi-CPP-1** (Fig. 4a, which is an experimental replicate of **Bi-CPP-1** shown in Fig. 2a) was again seen in some individual cells.

Average areal densities of bismuth in treated cells were elevated relative to controls (also replicated and analysed at the reduced XFM dwell time; see Fig. 7e), and consistent with the levels observed in all three treatments imaged at the longer dwell time. Extranuclear bismuth accumulation was also observed in some cells treated with the coumarin-appended peptides (Fig. 4b/c, S34 and S35).

In cells treated with the coumarin-labelled peptides (both brominated and non-brominated), there was moderate correlation between the bismuth signal and the optical fluorescence distribution from the coumarin emission channel. However, as noted for **Bi-CPP-1-Np** and **Bi-CPP-1-NpBr** (Fig. 2), fluorescence signals from coumarin were also observed in regions not associated with cell bodies or bismuth distribution (*e.g.*, Fig. 4b). The average cellular areal density of bromine in cells treated with **Bi-CPP-1-CouBr** was roughly two-fold elevated compared to

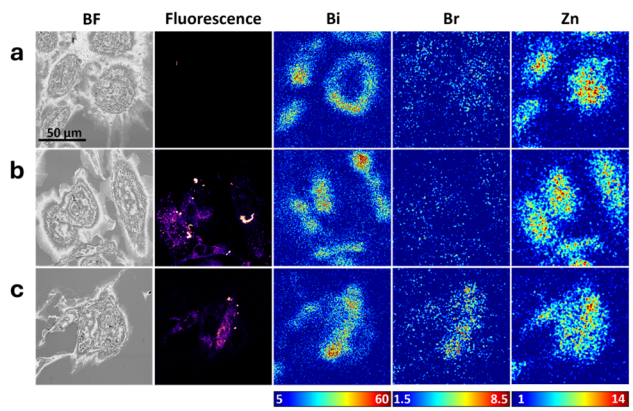

Fig. 4 Correlation of brightfield (BF), confocal optical fluorescence (coumarin) and XFM images (Bi, Br and Zn – false colour scale bars show areal density in ng cm^{-2}) for SKOV-3 cells treated with (a) **Bi-CPP-1**, (b) **Bi-CPP-1-Cou** and (c) **Bi-CPP-1-CouBr** (all treatments 10 μM, 4 h). Scale bar at top left (50 μm) applies to all images.

controls and treatments with non-brominated peptide conjugates (Fig. 7f). However, this elevation was less than expected based on the increase in bismuth in that treatment (nearly an order of magnitude) and was inconsistent with the bromine elevation observed in cells treated with either **Bi-CPP-1-NpBr** or **Bi-CPP-2-NpBr**. Collectively, these observations suggest that coumarin labelling of Bi-CPPs is less robust under these conditions compared to the stability observed with naphthalimide labelling. Furthermore, the data indicate that bromination was perturbed during cell treatment, which we attribute to a potential artifact, as the covalent bond between bromine and coumarin is expected to be stable.

Bi-CPP-1 and Bi-CPP-3 conjugated to rhodamine B analogues

Two final sets of labelled peptides were used to treat SKOV-3 cells, in which a rhodamine B fluorophore (brominated or non-brominated) was appended to either **Bi-CPP-1** (Fig. 5) or **Bi-CPP-3** (Fig. 6). **Bi-CPP-3** is a direct derivative of **Bi-CPP-1**, in which the duplicated C-terminal KRK motif is replaced by uncharged SGS residues. With only three basic residues, **Bi-CPP-3** is among the least basic CPPs reported to date.[2] Direct comparison of **Bi-CPP-1** and **Bi-CPP-3**, each bearing the same rhodamine B dye (or its brominated form), thus provided an additional opportunity to assess the importance of multiple *versus* fewer basic residues in Bi-CPPs. **Bi-CPP-1** and **Bi-CPP-3**, as well as their rhodamine B-labelled variants **Bi-CPP-1-RhB** and **Bi-CPP-3-RhB**, were previously investigated by us for cellular uptake in HeLa cells using live-cell confocal fluorescence microscopy, fluorescence-activated cell sorting and ICP-MS.[2] These studies indicated similarly efficient uptake, with a tendency toward increased uptake in the absence of the dye.

In the samples analysed in the current study in SKOV-3 cells (Fig. 5 and 6), consideration of the correlated multimodal images yields similar broad conclusions to those from the previous sets (Fig. 2–4). We observed elevations in cellular bismuth, bromine and rhodamine B signals with generally well-correlated distributions, suggesting cellular partitioning to a compartment or organelle adjacent to the cell nucleus as well as moderate, if imperfect, robustness of the peptide labelling.

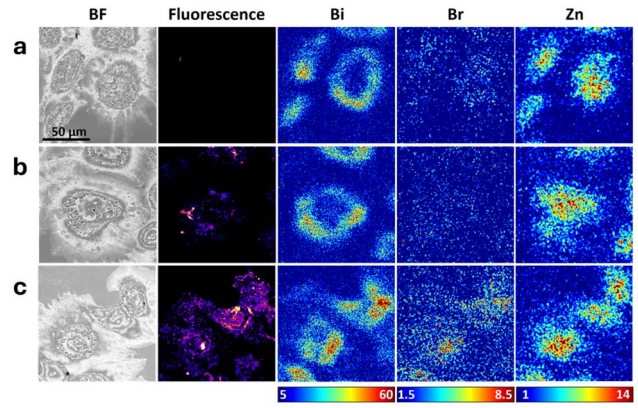

Fig. 5 Correlation of brightfield (BF), confocal optical fluorescence (rhodamine B) and XFM images (Bi, Br and Zn – false colour scale bars show areal density in ng cm^{-2}) for SKOV-3 cells treated with (a) **Bi-CPP-1** (repeated from Fig. 4a), (b) **Bi-CPP-1-RhB** and (c) **Bi-CPP-1-RhBBr** (all treatments 10 μM, 4 h). Scale bar at top left (50 μm) applies to all images.

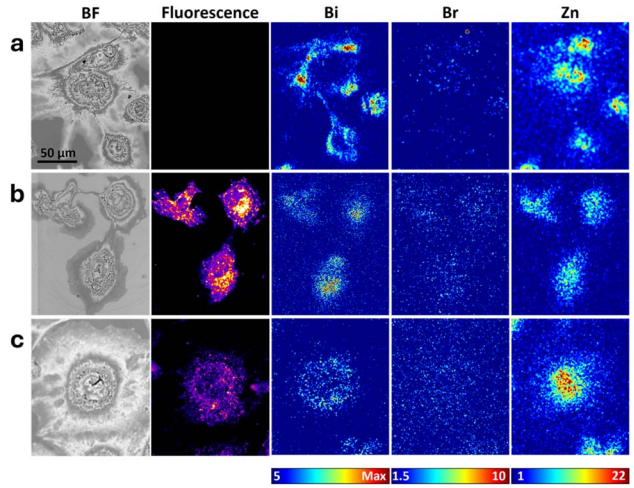

Fig. 6 Correlation of brightfield (BF), confocal optical fluorescence (rhodamine B) and XFM images (Bi, Br and Zn – false colour scale bars show areal density in ng cm^{-2}) for SKOV-3 cells treated with (a) **Bi-CPP-3**, (b) **Bi-CPP-3-RhB** and (c) **Bi-CPP-3-RhBBr** (all treatments 10 μM, 4 h). Scale bar at top left (50 μm) applies to all images. False colour intensity for XFM Bi maps is (a) 5–80 ng cm^{-2}, (b) 5–40 ng cm^{-2} and (c) 5–20 ng cm^{-2}.

Quantitation of the average areal density of bromine determined *via* XFM (Fig. 7j) potentially indicates poor stability of the labelling in the **Bi-CPP-3-RhBBr** conjugate, most notably in comparison to the **Bi-CPP-1** analogue (Fig. 7h), where bromine is elevated. However, we also note that both the bismuth and rhodamine B signals in these treated cells are markedly lower. As such, it may be that this conjugate, **Bi-CPP-3-RhBBr**, is not taken up by cells as efficiently as the other peptide conjugates examined in this study, which might be a consequence of its fewer basic residues, the brominated rhodamine B dye, or both. Overall, this trend is consistent with our previous observation that rhodamine B conjugation to Bi-CPPs appears to decrease cellular uptake.[2]

Limitations of imaging approach

Both imaging methods, X-ray fluorescence and optical fluorescence, detect signals arising from distinct moieties of each conjugate examined in this study. Our interpretation and conclusions rely on the assumption that a strong spatial correlation between these discrete signals indicates that the individual moieties remain attached within the conjugate under investigation. While it is theoretically possible that the conjugate could be degraded into separate components that are subsequently processed by the cell into the same subcellular compartments (resulting in apparent co-localisation), our experience, together with consideration of the likely divergent biological chemistry of potential degradation products, suggests that this scenario is unlikely. Nevertheless, a complementary approach to directly assess conjugate stability, such as

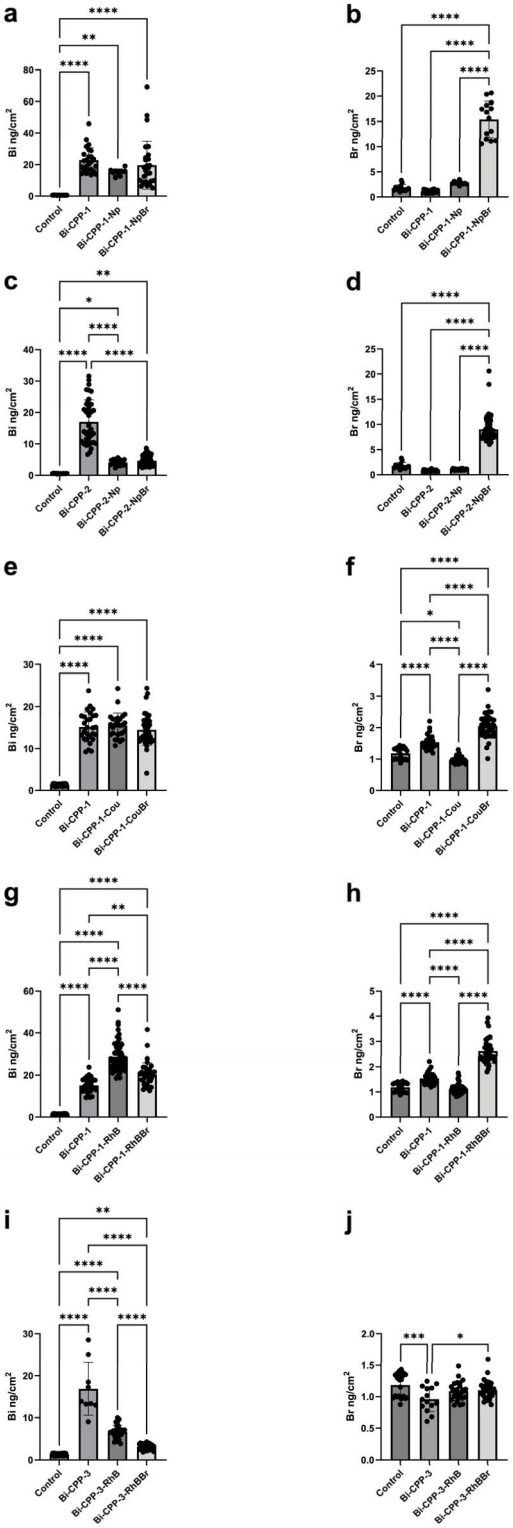

Fig. 7 Mean Bi (left panels a, c, e, g and i) and Br (right panels b, d, f, h and j) areal densities (ng cm^{-2}) of SKOV-3 cells after 4 h of incubation with all bismuth peptides investigated in this study (10 μM Bi-CPP, excepting controls). Statistical comparisons were achieved using an ordinary one-way ANOVA with a *post hoc* Tukey's multiple comparisons test with single pooled variance. Data represents mean ± SD. Notation *, **, ***, **** indicate $P < 0.05$, $P < 0.01$, $P < 0.001$, $P < 0.0001$, respectively. See SI for number of cells included in the analyses of each condition and details on software used.

HPLC-MS analysis of cell lysates, would provide increased confidence. While the sensitivity of the instrumentation currently available to us proved insufficient, we aim to pursue chromatography-mass spectrometry analyses in future studies.

Such future studies would also provide validation in cases where our multimodal imaging approach suggests conjugate degradation based on a loss of spatial correlation between signals from the different tags. While a loss of correlation between XRF signals (*i.e.*, bromine and bismuth) almost certainly indicates degradation of the conjugate, it is conceivable that a loss of correlation between XRF signals and the optical fluorophore could instead arise from fluorophore quenching due to an unrecognised cellular processing event.

The fixation protocol employed in this study has the potential to influence the cellular fate of the conjugates, either by altering their localisation or, less likely, their stability. Future studies may therefore assess the localisation of optically fluorophore-tagged conjugates in live cells and compare these results with those obtained in the present work.

Conclusions

This study presents the first report of trimodal probes enabling cellular detection and localisation of both bismuth and bromine *via* XFM alongside various fluorescent dyes for optical fluorescence microscopy. It also marks the first instance of simultaneous detection of bismuth and bromine in cells using XFM. Because bromine and bismuth are attached to the cell-penetrating peptide through entirely distinct chemical strategies, we were able, for the first time, to differentiate the fate of bismuth from that of the peptide and the fluorescent dye, allowing more nuanced insights into their cellular behaviour and stability. Co-localisation of bismuth, bromine and dye in multiple samples demonstrates that bismuth peptides can enter cells and remain presumably intact, advancing our previous studies[2] using ICP-MS or optical fluorophore tagging which showed uptake but could not prove stability of the conjugates. Our findings suggest that naphthalimide dyes and their brominated analogues perform most reliably for this type of multimodal imaging, and future study should assess this in different cell lines and in live cells (focusing on optical probe tags given that XRF is not compatible with live cells). Our study provides a valuable toolbox for the future development of bismuth peptides for biomedical applications.

Author contributions

Conceptualisation (EJN, HHH and CN), funding acquisition (EJN, HHH and CN), investigation (SV, CJK, LDA, TK, ATB, DH, SON and PP), supervision (EJN, HHH and CN), visualisation (CJK) and writing (HHH and CN).

Conflicts of interest

There are no conflicts to declare.

Data availability

The data supporting this article have been included as part of the supplementary information (SI). Supplementary information is available. See DOI: https://doi.org/10.1039/d5sc06490b.

Acknowledgements

The authors are grateful for funding provided by the Australian Research Council grants awarded to EJN, HHH and CN (DP210102148, DP230100079, FT220100010, CE200100012). Part of this research was undertaken on the X-ray Fluorescence Microscopy beamline at the Australian Synchrotron (Clayton, Victoria),[15] with merit beamtime funded by the Australian Nuclear Science and Technology Organisation (ANSTO). Optical imaging was conducted using instruments managed by Adelaide Microscopy (The University of Adelaide). We acknowledge the scientific and technical assistance of Sydney Analytical Core Research Facility at the University of Sydney. The authors wish to thank Dr Max J. Bedding, University of Sydney, for assistance with UPLC-MS. SV acknowledges Innovate UK (UKRI).

Notes and references

1 S. Voss, J. Rademann and C. Nitsche, *Angew. Chem., Int. Ed.*, 2022, **61**, e202113857.
2 S. Voss, L. D. Adair, K. Achazi, H. Kim, S. Bergemann, R. Bartenschlager, E. J. New, J. Rademann and C. Nitsche, *Angew. Chem., Int. Ed.*, 2024, **63**, e202318615.
3 J. L. Ritchey, L. Filippi, D. Ballard and D. Pei, *Mol. Pharmaceutics*, 2024, **21**, 5255–5260.
4 L. J. Davies, P. Ghosh, S. Siryer, S. Ullrich and C. Nitsche, *Chem.–Eur. J.*, 2025, **31**, e202500064.
5 S. Ullrich, U. Somathilake, M. Shang and C. Nitsche, *Commun. Chem.*, 2024, **7**, 143.
6 R.-N. He, M.-J. Zhang, B. Dai and X.-D. Kong, *ACS Chem. Biol.*, 2024, **19**, 1040–1044.
7 C. Heinis, T. Rutherford, S. Freund and G. Winter, *Nat. Chem. Biol.*, 2009, **5**, 502–507.
8 H. Krishna Sudhakar, J. T. K. Yau, L. J. Alcock and Y. H. Lau, *Org. Biomol. Chem.*, 2024, **22**, 6095–6102.
9 F. Bruchertseifer, A. Kellerbauer, R. Malmbeck and A. Morgenstern, *J. Labelled Compd. Radiopharm.*, 2019, **62**, 794–802.
10 C.-N. Tsang, K.-S. Ho, H. Sun and W.-T. Chan, *J. Am. Chem. Soc.*, 2011, **133**, 7355–7357.
11 M. E. Graziotto, C. J. Kidman, L. D. Adair, S. A. James, H. H. Harris and E. J. New, *Chem. Soc. Rev.*, 2023, **52**, 8295–8318.
12 Z. Qian, T. Liu, Y.-Y. Liu, R. Briesewitz, A. M. Barrios, S. M. Jhiang and D. Pei, *ACS Chem. Biol.*, 2013, **8**, 423–431.
13 L. D. Adair, M. E. Graziotto, T. Koh, C. J. Kidman, B. J. Schwehr, M. J. Hackett, M. Massi, H. H. Harris and E. J. New, *Chem. Commun.*, 2024, **60**, 9026–9029.
14 J. H. Lovett, B. P. Lai, H. O. Bloomfield, A. T. Baker, M. P. Sullivan, C. G. Hartinger and H. H. Harris, *Chem. Sci.*, 2025, **16**, 11347–11358.
15 D. L. Howard, M. D. de Jonge, N. Afshar, C. G. Ryan, R. Kirkham, J. Reinhardt, C. M. Kewish, J. McKinlay, A. Walsh, J. Divitcos, N. Basten, L. Adamson, T. Fiala, L. Sammut and D. J. Paterson, *J. Synchrotron Radiat.*, 2020, **27**, 1447–1458.